

Communication

Not peer-reviewed version

Valley-Spin-Polarization of MoS₂ Monolayer Induced by Ferromagnetic Order in an Antiferromagnet

Chun-Wen Chan , Chia-Yun Hsieh , Fang-Mei Chan , Pin-Jia Huang , [and Chao-Yao Yang](#) *

Posted Date: 18 July 2024

doi: 10.20944/preprints202407.1480.v1

Keywords: molybdenum disulfide; valleytronics; antiferromagnet; magnetic proximity effect



Preprints.org is a free multidiscipline platform providing preprint service that is dedicated to making early versions of research outputs permanently available and citable. Preprints posted at Preprints.org appear in Web of Science, Crossref, Google Scholar, Scilit, Europe PMC.

Copyright: This is an open access article distributed under the Creative Commons Attribution License which permits unrestricted use, distribution, and reproduction in any medium, provided the original work is properly cited.

Disclaimer/Publisher's Note: The statements, opinions, and data contained in all publications are solely those of the individual author(s) and contributor(s) and not of MDPI and/or the editor(s). MDPI and/or the editor(s) disclaim responsibility for any injury to people or property resulting from any ideas, methods, instructions, or products referred to in the content.

Communication

Valley-Spin-Polarization of MoS₂ Monolayer Induced by Ferromagnetic Order in an Antiferromagnet

Chun-Wen Chan ¹, Chia-Yun Hsieh ¹, Fang-Mei Chan ¹, Pin-Jia Huang ¹ and Chao-Yao Yang ^{1,2,*}

¹ Department of Materials Science and Engineering, National Yang Ming Chiao Tung University, Hsinchu, 300093, Taiwan; henrieqiut@gmail.com

² Center for Emergent Functional Matter Science, National Yang Ming Chiao Tung University, Hsinchu 300093, Taiwan

* Correspondence: cyyang8611@nycu.edu.tw

Abstract: Transition metal dichalcogenides (TMDs) monolayers exhibit unique valleytronics properties due to the dependency of the coupled valley and spin state at the hexagonal corner of the first Brillouin zone. Precisely controlling valley spin-polarization via manipulating the electron population enables its application in valley-based memory or quantum technologies. This study uncovered the uncompensated spins of the antiferromagnetic oxide (NiO) serving as the ferromagnetic (FM) order to induce valley spin-polarization in molybdenum disulfide (MoS₂) monolayers via the magnetic proximity effect (MPE). A spin-resolved photoluminescence spectroscopy (SR-PL) was employed to observe MoS₂, where the spin-polarized trions appear to be responsible for the MPE, leading to a valley magnetism. Results indicate that local FM order from the uncompensated surface of NiO could successfully induce significant valley spin-polarization in MoS₂ with the depolarization temperature approximately at 100 K, which is relatively high compared to related literature. This study reveals new perspectives and potential of AFM materials in the field of exchange-coupled van der Waals heterostructures.

Keywords: molybdenum disulfide; valleytronics; antiferromagnet; magnetic proximity effect

1. Introduction

Transition metal dichalcogenides (TMDs) feature a layered structure similar to graphene but with a direct bandgap, making them ideal semiconductor candidates for various applications [1–3]. Structurally, TMDs can adopt three different crystalline forms: 1T, 2H, and 3R. Both the 2H and 3R phases exhibit trigonal prismatic coordination and are naturally semiconductors, but the 2H structure is more thermally stable than the 3R, making it more suitable for applications requiring stability [4–6]. The crystal structure of a TMD monolayer belongs to the hexagonal crystal system, and its reciprocal space exhibits six-fold symmetry [7,8]. When the thickness of TMDs is reduced to a monolayer, the lack of inversion symmetry gives rise to the valley degeneracy in the reciprocal space to split into inequivalent K and K' points with opposite spin states [9–11]. This valley-spintronic effect makes the electron spin and valley properties interdependent and sensitive to the lights with angular momentum [7,9,12]. When specific circularly polarized light (either left- or right-handed) is incident on the TMD monolayer, it spin-dependently excites electrons in a specific valley, leading to different occupation levels in the two valleys and resulting in valley spin-polarization [13]. This spin-dependent electron transition mechanism, by controlling valley properties, influences the optoelectronic and magnetic properties of TMDs and has given rise to a new research field known as valleytronics. Recent studies have explored various approaches to induce valley spin-polarization, such as using circularly polarized light for photoexcitation [9,14,15] and the Zeeman effect in

magnetic fields to break spin symmetry [16–18]. It has been observed that valley spin-polarization can be triggered via the magnetic proximity effect (MPE) of ferromagnetic (FM) materials, which can be achieved at accessible field levels below 1 Tesla, as demonstrated by spin-sensitive spectroscopy [19–21]. These findings provide possibilities for realizing TMD-based valley spintronics for more diverse applications. Although the MPE-induced valley spin-polarization in TMD monolayers is clear, an intriguing but unresolved question remains: Can the ferromagnetic order in antiferromagnets enable the MPE in TMD monolayers to incorporate more ingredients into future valleytronics? This issue is promising but requires a more comprehensive understanding.

This study attempts to resolve the magnetic proximity effect (MPE) induced by an antiferromagnet (AFM) NiO with a specific crystallographic orientation. NiO is a G-type AFM with a Néel temperature higher than room temperature [22,23]. It has been shown that the (111)-terminated surface of NiO can host the MPE with a depolarization temperature at approximately 100 K, while the (001)-terminated surface of NiO dramatically deactivates the MPE. This phenomenon revisits the importance of the FM order in AFM through uncompensated spins. This approach provides a new perspective on the study of magnetic van der Waals heterostructures using AFM materials.

2. Materials and Methods

In this study, a three-zone tube furnace was used for chemical vapor deposition (CVD) to grow monolayer MoS₂ on a sapphire substrate. The molybdenum trioxide (MoO₃) powders and sulfur (S) powders were used as precursors, positioned in the middle of the second zone and the front end of the first zone, respectively. The sapphire substrates were placed downstream of the MoO₃ at the second zone. An argon atmosphere with a flow rate of 40 sccm was applied as the carrier gas to promote the reaction of MoO₃ and S and the subsequent deposition onto sapphire substrates. During the CVD, the pressure inside the tube furnace was maintained at 4 torr. The set temperatures at the zone 1, 2, and 3, are 550 °C, 750 °C, and 800 °C, respectively. This creates a temperature gradient inside the tube, promoting the deposition with different distances from MoO₃ at zone 2. After growing MoS₂ monolayers on a sapphire substrate, a wet transfer technique was used to transfer the MoS₂ samples onto the desired NiO substrates with (111)-terminated and (001)-terminated surface. Polymethyl methacrylate (PMMA) was spin-coated onto the sapphire substrate with the grown MoS₂ monolayers. After a soft bake treatment at 120°C for 2 minutes, the sample was soaked in a 1M potassium hydroxide solution for 30 minutes, and then immersed in deionized water for cleaning. Due to the hydrophobic nature of PMMA, the PMMA adhered to MoS₂ would lift off from the sapphire substrate and be transferred onto the surface of NiO with specific surface termination. The desired substrate is then used to pick up the PMMA/MoS₂ film. After drying, the sample is soaked in acetone for 2 hours to remove the PMMA, thus completing the transfer process for subsequent characterizations. The Raman and photoluminescence (PL) spectra were collected using a Raman spectrometer with an argon laser source of 533 nm at room temperature. The laser beam was focused onto the sample's surface and the spot size was approximately 1 μm. The laser current was 0.755 A, and a 1200-line/mm grating was employed for an energy resolution of 2 meV. The integration time for collecting Raman and PL spectra was 30 and 5 seconds to yield distinguishable signals, respectively. Spin-resolved PL (SR-PL) was performed using linearly polarized light to pump and circularly polarized lights to probe the MoS₂ monolayers on the NiO substrate at various temperatures.

3. Results

Figure 1a shows the morphology of the MoS₂ grown on the sapphire substrate, in which the MoS₂ domains appear to be randomly distributed and orientated on the sapphire substrate. It reveals the sapphire substrate is atomically flat, thus lacking the preferred nucleation sites on the sapphire surface during the deposition. Figure 1b exhibits the Raman spectrum acquired from the MoS₂ domain as demonstrated in Figure 1a. The two characteristic peaks at ~384 cm⁻¹ (E_{2g}^1) and ~403 cm⁻¹ (A_{1g}) correspond to the horizontal and vertical vibration modes of the MoS₂ monolayer. The

monolayer nature of the grown MoS₂ is indicated by the wave number difference between E_{2g}^1 and A_{1g} , approximately 19 cm⁻¹ [24,25]. An atomic force microscope (AFM) was employed to probe the step height at the edge of MoS₂ to examine the properties of the monolayer for the associated valleytronics properties. Figure 1c shows the topography of MoS₂ grown on the sapphire substrate, and Figure 1d shows the step profile of the investigated MoS₂ probed along the scanning trajectory, as shown by the blue line in Figure 1c. As a result, the step height is approximately 0.74 nm, suggesting the MoS₂ in the form of monolayer fabricated by CVD.

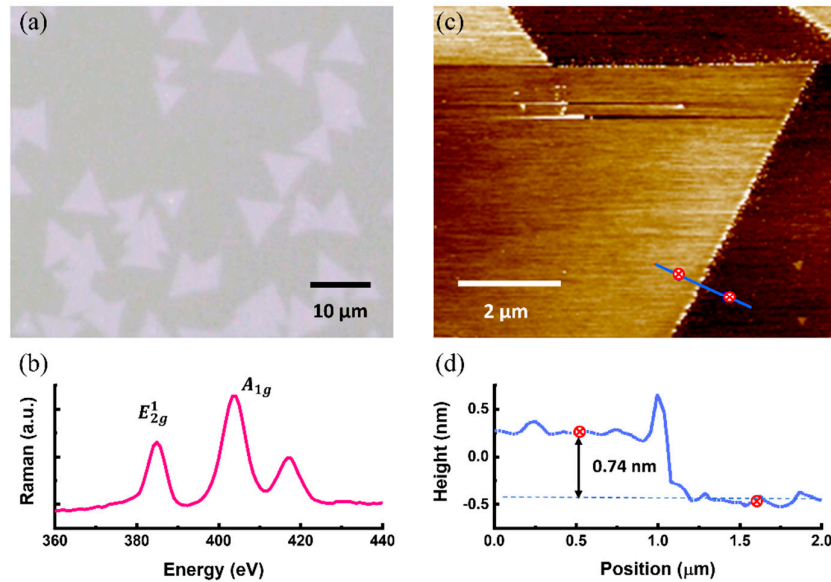


Figure 1. (a) Optical microscope image of the MoS₂ monolayers distributed on the sapphire surface. (b) Raman spectrum acquired by the MoS₂ monolayer in (a). (c) Topographic image of MoS₂ monolayer taken by an atomic force microscope together with (d) step height of approximately 0.744 nm taken at its edge as marked by the blue line.

After the fabrication of the MoS₂ monolayers and the characterization, the focus was turned to the effect of transferring MoS₂ monolayers onto the NiO substrate. Figure 2a shows the crystal and magnetic structure of the NiO, featuring a rock-salt structure with the AFM texture in a G-type configuration [26,27]. Based on the magneto-structural configuration, the NiO with (111) termination yields a significant FM order on the surface as an uncompensated plane. On the contrary, the NiO with (001) termination is magnetically compensated, resulting in no considerable magnetization on the surface and serving as the natural AFM order in NiO. Figure 2b shows the Raman spectra before and after the MoS₂ transfer onto the NiO substrate with (111) termination, denoted as NiO₍₁₁₁₎, in which the E_{2g}^1 state didn't vary notably but the A_{1g} state appeared to be softened after the transfer. Based on the current literature, the E_{2g}^1 state is relatively sensitive to the strain/stress issue arising from the different interfacial coherency with the substrate, therefore, the transfer treatment gave rise to limited strain issues. However, the A_{1g} softening suggests the electron doping effect arising from the charge transfer from the substrate [12,28–30]. The result suggests that interfacing MoS₂ with NiO would stabilize the n-type characteristic of MoS₂. Furthermore, the PL spectra before and after the MoS₂ transfer both reflect the exciton state ~1.83 eV as an indicator of the high monolayer quality [31], but it shows the PL red-shifting ~10 meV upon transferring the MoS₂ monolayers onto the NiO₍₁₁₁₎. Both Raman and PL spectra suggest the MoS₂ on NiO₍₁₁₁₎ indeed underwent an electronic transition after the transfer. A detailed discussion regarding the electronic modification on MPE will be provided after having the results of SR-PL characterization.

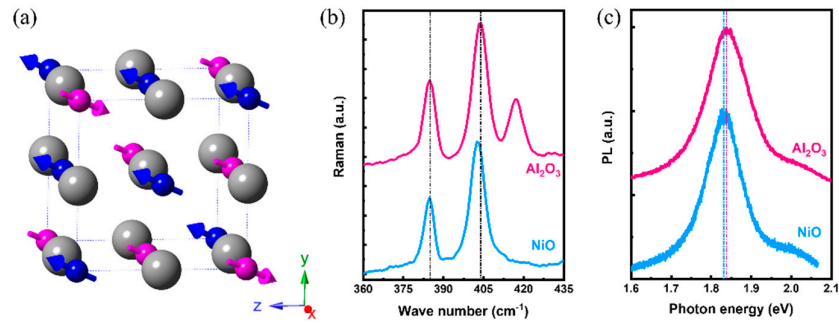


Figure 2. (a) Crystal and magnetic structure of NiO substrate exhibiting the rock-salt structure and the G-type AFM texture, respectively. The FM and AFM orders of NiO can be observed on the (111)-terminated and (001)-terminated surfaces, corresponding to the uncompensated and compensated plane of NiO. (b) Raman spectra and (c) PL spectra acquired from the MoS₂ monolayers on Al₂O₃ and NiO₍₁₁₁₎ substrate.

Figure 3a shows the SR-PL spectra of MoS₂ on NiO₍₁₁₁₎ with temperature dependency, probed using the right-handed (RCP) and left-handed (LCP) circularly polarized lights. SR-PL taken at 4 K exhibited two distinguishable states at 1.93 eV and 1.97 eV corresponding to the trion and exciton states, denoted as T and A, respectively. As the results, the SP-PL taken at 4 K exhibits a distinguishable magnetic circular dichroism (MCD) at both T and A states, suggesting the valley spin-polarization in the MoS₂ monolayers triggered by the MPE of NiO₍₁₁₁₎ substrate. It could be noticed that both T and A states underwent a redshift transition upon increasing the temperature. It is because of the thermal expansion driving electrical band gap reduction, thus reducing the optical band gap [32,33]. In addition, it has been shown both T and A states are responsible for the valley spin-polarization while putting the MoS₂ monolayers on NiO₍₁₁₁₎. Figure 3b exhibits the SR-PL results of the control sample comprising MoS₂ monolayers on NiO₍₀₀₁₎. As expected, the NiO₍₀₀₁₎ has a fully spin-compensated surface, thus resulting in no distinguishable MCD via the probe of SR-PL. Comparing the results in Figure 3a,b, it reveals the crystallographic control of the AFM NiO substrate appears to be a critical switch to induce the valley spin-polarization via MPE. Figure 3c exhibits the plots of the degrees of the valley spin-polarization for the T and A states of the MoS₂ monolayers on NiO₍₁₁₁₎ and the A state of the MoS₂ monolayers on NiO₍₀₀₁₎. It shows the depolarization of the T and A states acquired by the MoS₂ monolayers on NiO₍₁₁₁₎ is roughly at 100 K, which is relatively high in the associated studies [19,34]. Besides, the valley spin-polarization degree mismatch among the T (NiO₍₁₁₁₎), T (NiO₍₁₁₁₎), and the A (NiO₍₀₀₁₎) at 4 K may reveal two important signatures: (1) The (111)-terminated surface of NiO substrate enables activating the MPE as a crystallographic switch. (2) T state appears to be much more sensitive to the MPE, hence giving rise to the higher valley spin-polarization degree. In order to explain the latter observation, a charge-transfer-induced MPE is introduced together with the origin of the valley spin-polarization.

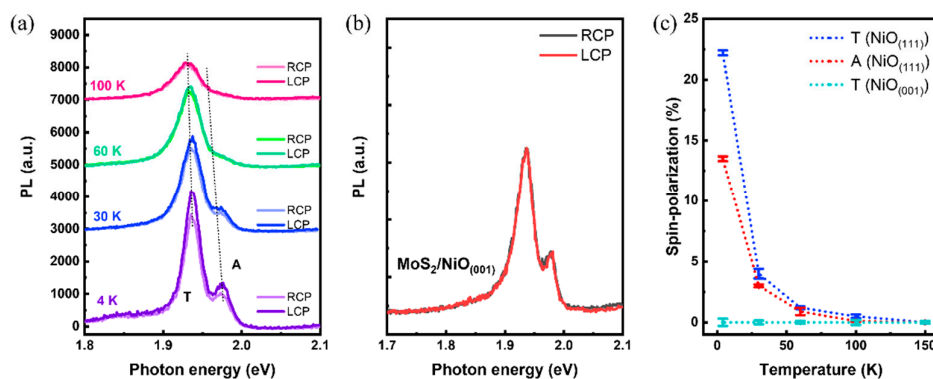


Figure 3. (a) SR-PL spectra of MoS₂ monolayers on NiO(111) taken at various temperatures. (b) SR-PL spectra of MoS₂ monolayers on NiO(001) taken at 4 K. (c) Plots of the degrees of valley spin-polarization at T and A states acquired from the MoS₂ monolayers on NiO(111) and NiO(001) at various temperature to reveal the depolarization temperature.

Let's revisit the SR-PL results and discuss the origin of the MPE based on the spin configuration in the MoS₂/NiO heterostructure. As shown in Figure 3a, both T and A states existed at low temperatures (<100 K) and it should be noticed that the T state is much correlated with magnetism. Figure 4a conceptually depicts the magnetism associated with the T state, in which the spins carried by the electron and hole located in the K valley and the spin carried by the electron in the K' valley are exhibited. Consequently, the spins carried by the electron and hole located in the K valley would compensate each other in nature, thus resulting in no magnetism. However, the additional spin located in the K' valley yields the net moment. The T states highlighted by the blue and red triangle shadows represent the local net moments with spin up and spin down, denoted as T(↑) and T(↓), respectively. In general, both T(↑) and T(↓) should populate equally and therefore leading to no magnetism. However, once the MoS₂ monolayers interface with the NiO with (111) termination, the interfacial exchange coupling between MoS₂ and NiO(111) would favor one of the T states and induce the imbalanced T population on the net valley spin-polarization. On the counterpart, upon interfacing MoS₂ monolayers with NiO(001), the fully compensated surface, as shown in Figure 4b, would result in no population preference on the T state, therefore deactivating the MPE to diminish the valley spin-polarization. This observation suggests precise control over the crystallographic growth of AFM functions as an effective switch to activate the MPE in MoS₂ monolayers, which is not only scientifically interesting but also practical for valley spintronics.

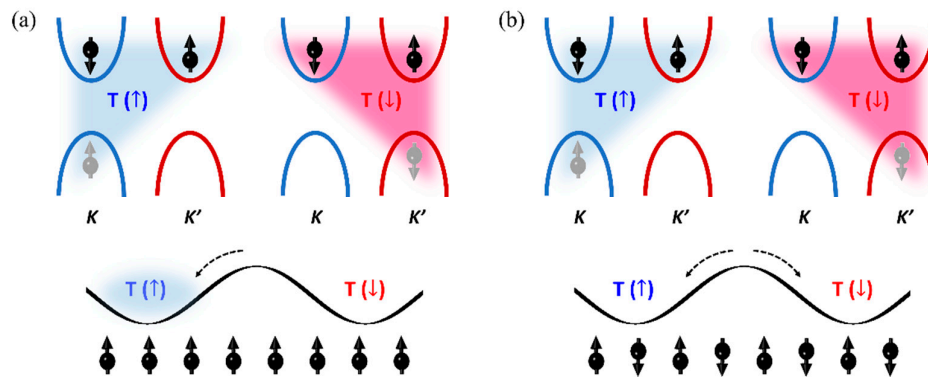


Figure 4. Schematic diagram to demonstrate the spin configuration of trion with (a) MPE-induced valley spin-polarization via preferred population to T(↑) driven by (111)-terminated NiO surface and (b) neutral population driven by (001)-terminated NiO surface. .

4. Discussion

Although the MPE has been observed on the (111)-terminated NiO surface, there are still two issues regarding the exchange coupling and the depolarization temperature on the T state. Because the uncompensated spins on NiO surface cannot be easily determined by the external field, the sign of the MPE-induced valley spin-polarization should reveal the information of the uncompensated spins on the NiO. Based on this perspective, the element-specific probe utilizing an X-ray magnetic circular dichroism may allow for resolving the exchange coupling at the interface. Therefore, the sign of magnetic dichroism in SR-PL may reciprocally help reconstruct the surface magnetism of NiO, which is conventionally challenging. In addition, the T state is not as sustainable as the A state upon increasing the temperature. The intervalley scattering on the trion state would be even more profound at the ramped temperature condition, thus leading to the drop in the valley spin-polarization together with the broadening of the SR-PL spectra. The results suggest using a time-resolved SR-PL may further study the MPE-associated properties via the kinetics dimension.

Minimizing the scattering on the T state may increase its lifetime and may potentially stabilize the valley spin-polarization at a relatively higher temperature, i.e. >100 K. That is, the ultrafast pump-probe technique should enable studying these MPE-associated issues in the MoS₂ monolayers for future applications.

5. Conclusions

In this work, the MPE-induced valley spin-polarization in the MoS₂ monolayers has been uncovered while interfacing the MoS₂ monolayers with a (111)-terminated NiO substrate studied by utilizing an SR-PL spectroscopy. On the (111)-terminated NiO surface, the depolarization temperature of the MoS₂ monolayers appears to be at around 100 K. Contrary, the (001)-terminated NiO substrate hasn't been seen with the MPE effect even though at the basal temperature at 4 K. The results suggest the precise control over the surface termination for the NiO substrate functions as a crystallographic switch to activate the MPE in the MoS₂ monolayers adjacent. Electronically, it appears the MPE-induced spin-polarized T state should result from the preferred T population, which naturally carries the local magnetism in the specific valley. Valley kinetics of trions and excitons responsible for the observed MPE should be studied in the next stage to promote MoS₂-based valley spintronics applications.

Author Contributions: This study was conceptually conceived by CYY. PJH fabricated the MoS₂ samples and did the wet transfer to NiO substrates. CWC helped with the spectroscopy measurements with the assistance of FMC. CWC and CYH organized the paper and drafted the manuscript under the supervision of CYY. All the authors commented on the manuscript. All authors have read and agreed to the published version of the manuscript.

Funding: This research is supported by the National Science and Technology Council of Taiwan (NSTC) under grant NSTC-112-2112-M-A49-026 and was also supported by the Higher Education Sprout Project and Center for Emergent Functional Matter Science of National Yang Ming Chiao Tung University from The Featured Areas Research Center Program within the framework of the Higher Education Sprout Project by the Ministry of Education (MOE) in Taiwan.

Institutional Review Board Statement: Not applicable.

Informed Consent Statement: Not applicable.

Data Availability Statement: The authors declare that the main data supporting the findings of this study are available within the article. Extra data are available from the corresponding author upon reasonable request.

Acknowledgments: The authors would like to thank the support of SR-PL measurements from Prof. Wen-Hao Chang's group at Dept. Electrophysics, National Yang Ming Chiao Tung University.

Conflicts of Interest: The authors declare no competing interests.

References

1. Khatei, J., Ojha, B. & Samal, D. Valleytronics. *Resonance* **2023**, *28*, 537-546.
2. Schaibley, J. R. *et al.* Valleytronics in 2D materials. *Nature Reviews Materials* **2016**, *1*
3. Liu, Y. *et al.* Valleytronics in transition metal dichalcogenides materials. *Nano Research* **2019**, *12*, 2695-2711.
4. Thomas, N. *et al.* 2D MoS₂: structure, mechanisms, and photocatalytic applications. *Materials Today Sustainability* **2021**, *13*
5. Wang, R. *et al.* Strategies on Phase Control in Transition Metal Dichalcogenides. *Advanced Functional Materials* **2018**, *28*
6. Yang, C.-Y. *et al.* Phase-driven magneto-electrical characteristics of single-layer MoS₂. *Nanoscale* **2016**, *8*, 5627-5633.
7. Bussolotti, F. *et al.* Roadmap on finding chiral valleys: screening 2D materials for valleytronics. *Nano Futures* **2018**, *2*
8. Lu, Z. *et al.* Magnetic field mixing and splitting of bright and dark excitons in monolayer MoSe₂. *2D Materials* **2019**, *7*
9. Mak, K. F., He, K., Shan, J. & Heinz, T. F. Control of valley polarization in monolayer MoS₂ by optical helicity. *Nat Nanotechnol* **2012**, *7*, 494-498.
10. Zhao, S. *et al.* Valley manipulation in monolayer transition metal dichalcogenides and their hybrid systems: status and challenges. *Rep Prog Phys* **2021**, *84*, 026401.

11. Zhu, Z. Y., Cheng, Y. C. & Schwingenschlögl, U. Giant spin-orbit-induced spin splitting in two-dimensional transition-metal dichalcogenide semiconductors. *Physical Review B* **2011**, 84
12. Huang, L. *et al.* Enhanced light-matter interaction in two-dimensional transition metal dichalcogenides. *Rep Prog Phys* **2022**, 85
13. Zeng, H. & Cui, X. An optical spectroscopic study on two-dimensional group-VI transition metal dichalcogenides. *Chem Soc Rev* **2015**, 44, 2629-2642.
14. Zeng, H., Dai, J., Yao, W., Xiao, D. & Cui, X. Valley polarization in MoS₂ monolayers by optical pumping. *Nat Nanotechnol* **2012**, 7, 490-493.
15. Kioseoglou, G. *et al.* Valley polarization and intervalley scattering in monolayer MoS₂. *Applied Physics Letters* **2012**, 101
16. Aivazian, G. *et al.* Magnetic control of valley pseudospin in monolayer WSe₂. *Nature Physics* **2015**, 11, 148-152.
17. Stier, A. V., McCreary, K. M., Jonker, B. T., Kono, J. & Crooker, S. A. Exciton diamagnetic shifts and valley Zeeman effects in monolayer WS₂ and MoS₂ to 65 Tesla. *Nat Commun* **2016**, 7, 10643.
18. Van der Donck, M., Zarenia, M. & Peeters, F. M. Strong valley Zeeman effect of dark excitons in monolayer transition metal dichalcogenides in a tilted magnetic field. *Physical Review B* **2018**, 97
19. Zhao, C. *et al.* Enhanced valley splitting in monolayer WSe₂ due to magnetic exchange field. *Nat Nanotechnol* **2017**, 12, 757-762.
20. Lyons, T. P. *et al.* Interplay between spin proximity effect and charge-dependent exciton dynamics in MoSe₂/CrBr₃ van der Waals heterostructures. *Nature Communications* **2020**, 11, 6021.
21. Seyler, K. L. *et al.* Valley manipulation by optically tuning the magnetic proximity effect in WSe₂/CrI₃ heterostructures. *Nano letters* **2018**, 18, 3823-3828.
22. Chatterji, T., McIntyre, G. J. & Lindgard, P. A. Antiferromagnetic phase transition and spin correlations in NiO. *Physical Review B* **2009**, 79, 172403.
23. Alders, D. *et al.* Temperature and thickness dependence of magnetic moments in NiO epitaxial films. *Physical Review B* **1998**, 57, 11623-11631.
24. Withanage, S. S., Lopez, M., Sameen, W., Charles, V. & Khondaker, S. I. Elucidation of the growth mechanism of MoS₂ during the CVD process. *MRS Advances* **2019**, 4, 581-586.
25. Li, T. *et al.* Epitaxial growth of wafer-scale molybdenum disulfide semiconductor single crystals on sapphire. *Nat Nanotechnol* **2021**, 16, 1201-1207.
26. Zhang, Y.-J., Luo, Y.-D., Lin, Y.-H. & Nan, C.-W. Anisotropic ferromagnetic behaviors in highly orientated epitaxial NiO-based thin films. *AIP Advances* **2015**, 5
27. Solovyev, I. V. Exchange interactions and magnetic force theorem. *Physical Review B* **2021**, 103
28. Chakraborty, B. *et al.* Symmetry-dependent phonon renormalization in monolayer MoS₂ transistor. *Physical Review B* **2012**, 85
29. Wu, L. *et al.* Raman scattering investigation of twisted WS₂/MoS₂ heterostructures: interlayer mechanical coupling versus charge transfer. *Nano Research* **2021**, 14, 2215-2223.
30. Yu, Y. *et al.* Engineering Substrate Interactions for High Luminescence Efficiency of Transition-Metal Dichalcogenide Monolayers. *Advanced Functional Materials* **2016**, 26, 4733-4739.
31. Sharma, M., Singh, A. & Singh, R. Monolayer MoS₂ Transferred on Arbitrary Substrates for Potential Use in Flexible Electronics. *ACS Applied Nano Materials* **2020**, 3, 4445-4453.
32. Xu, L. *et al.* Analysis of photoluminescence behavior of high-quality single-layer MoS₂. *Nano Research* **2019**, 12, 1619-1624.
33. Pei, J. *et al.* Exciton and trion dynamics in bilayer MoS₂. *Small* **2015**, 11, 6384-6390.
34. Zhang, Y. *et al.* Controllable Magnetic Proximity Effect and Charge Transfer in 2D Semiconductor and Double-Layered Perovskite Manganese Oxide van der Waals Heterostructure. *Adv Mater* **2020**, 32, e2003501.

Disclaimer/Publisher's Note: The statements, opinions and data contained in all publications are solely those of the individual author(s) and contributor(s) and not of MDPI and/or the editor(s). MDPI and/or the editor(s) disclaim responsibility for any injury to people or property resulting from any ideas, methods, instructions or products referred to in the content.